

The **next generation** GBCA
from Guerbet is here

Explore new possibilities >

Guerbet | 

© Guerbet 2024 GUOB220151-A

AJNR

Aneurysm Flow Dynamics: Alterations of Slipstream Flow for Neuroendovascular Treatment with Liquid Embolic Agents

Steven G. Imbesi, Kimberly Knox and Charles W. Kerber

AJNR Am J Neuroradiol 2003, 24 (10) 2044-2049

<http://www.ajnr.org/content/24/10/2044>

This information is current as
of July 2, 2024.

Aneurysm Flow Dynamics: Alterations of Slipstream Flow for Neuroendovascular Treatment with Liquid Embolic Agents

Steven G. Imbesi, Kimberly Knox, and Charles W. Kerber

BACKGROUND AND PURPOSE: The main issue with use of a liquid embolic agent is one of safety. To determine and improve the efficacy of potential neuroendovascular treatment regimens, particularly the use of liquid embolic agents, we evaluated the changes in aneurysm flow dynamics resulting from alterations of parent vessel flow.

METHODS: We created silicone replicas of a laboratory-created aneurysm model and a basilar artery aneurysm cast from a human cadaver. Replicas were placed in a circuit of pulsatile non-Newtonian fluid, and flows were adjusted to simulate human physiologic flow velocity, profile, and volume. Individual fluid slipstreams were opacified with isobaric dyes. Images were obtained of the unaltered vascular replica; after placement of a nondetachable balloon in the parent vessel at multiple locations proximal to, across, and distal to the aneurysm neck; and after placement of a stent across the aneurysm neck. Aneurysms were then occluded with a cyanoacrylate liquid embolic agent in association with each device.

RESULTS: In the unaltered replica, flow entered the distal aneurysm neck and impacted against the distal lateral aneurysm wall. Disturbed, but nonturbulent, flow then continued along the aneurysm wall in a vortex pattern and exited at the proximal aspect of the aneurysm neck. With the balloon partially inflated in the parent vessel, the slipstream velocity increased. This resulted in more rapid flow in the aneurysm sac, a less favorable condition for deposition of liquid embolic material. The effect was more pronounced with greater degrees of balloon inflation (resulting in greater parent vessel narrowing) and when the balloon was proximal to the aneurysm neck compared with more distal parent vessel positioning. Only with complete occlusion of the parent vessel lumen, either proximal to, across, or distal to the aneurysm sac, was there intraaneurysmal flow reduction (ie, stasis), a more favorable condition for liquid embolic material deposition. Also, with the balloon positioned across the aneurysm neck, not only did the liquid agent remain in the aneurysm sac, but also the surface could be molded to re-create a normal parent vessel lumen. A stent placed across the aneurysm neck caused the slipstreams to lose their coherence as they passed through the stent mesh. This prevented slipstream impact against the aneurysm sidewall and decreased the intraaneurysmal fluid velocity. During deposition of liquid embolic agent through the stent sidewall into the aneurysm sac, the stent mesh appeared to provide a barrier to passage of the embolic agent into the adjacent parent vessel, also a more favorable condition for liquid embolic material deposition.

CONCLUSION: Knowledge of aneurysm flow dynamics and the changes incurred after endovascular parent vessel flow alteration provides a basis for safer aneurysm obliteration by using a liquid embolic agent with a neurointerventional technique.

Currently, the only device approved by the U.S. Food and Drug Administration for the endovascular obliteration of an aneurysm sac is the platinum detachable coil (1). Although this has revolutionized the treatment of intracranial aneurysms, incomplete occlusion

or recanalization of the aneurysm sac is occasionally noted (2, 3). In general, incomplete occlusion (incomplete aneurysm sac packing) usually occurs in aneurysms with a wide neck owing to fear of coil prolapse into the adjacent parent vessel. Aneurysm sac recan-

Received March 7, 2003; accepted after revision June 17.

From the Department of Radiology, University of California, San Diego Medical Center, CA (all authors).

Presented at the 40th annual meeting of the American Society of Neuroradiology, Vancouver, BC, May 11–17, 2002.

Address reprint requests to Steven G. Imbesi, MD, Department of Radiology, University of California, San Diego Medical Center, 200 W. Arbor Dr., Mail Code #8756, San Diego, CA 92103.

© American Society of Neuroradiology

alization most often develops when the slipstream flow from the adjacent parent vessel directly impacts against the coil mass such as in a basilar tip aneurysm. Both of these problems are also more common in the larger aneurysm sacs (4). Other embolization agents need to be developed that are noncompressible, more permanent devices.

Use of cyanoacrylate cement for the intravascular occlusion of vessels has been performed for many years in the treatment of arteriovenous malformations. This agent has proved to be an efficacious and permanent occlusion device (5, 6). Thus, deposition of cyanoacrylate polymer in an aneurysm sac should result in better, more permanent aneurysm obliteration. The main issue with use of a liquid embolic agent is one of safety. However, in conjunction with a parent vessel protection device, a liquid agent could potentially be deposited safely and may also allow occlusion of the presently difficult to treat wide-necked aneurysm.

Flow dynamics of the intracranial circulation, and in particular of intracranial aneurysms, have been previously studied and described by using laboratory created models and actual human vascular casts (7–10). Use of these vascular replicas provides a unique opportunity to study the safety and efficacy of various aneurysm treatment strategies without patient risk. We studied a laboratory-created model, as well as an in situ casting of the brain arteries of a patient who had died of a ruptured intracranial aneurysm. We now report the results of those experiments.

Methods

Two types of aneurysm replicas were studied. First, a laboratory-created, clear elastic silicone model of a lateral sidewall aneurysm 1 cm in length with a wide neck of 5 mm was tested. Four identical copies were used: three for occlusion in conjunction with a nondetachable balloon and one for occlusion in conjunction with a vascular stent. The flow dynamics of each model was documented before treatment, after placement of the parent vessel protection device, and after deposition of the cyanoacrylate liquid embolic agent. Of note, regarding the parent vessel protection device, although the change in flow could only be evaluated with the stent positioned completely across the aneurysm neck (the single appropriate placement), the change in flow after nondetachable balloon placement was determined with the balloon positioned proximal to, across, and distal to the aneurysm neck, as well as with varying degrees of inflation.

Then the same experimentation was repeated by using an anthropomorphic vascular cast from a human cadaveric specimen; the patient had died of aneurysm rupture. The aneurysm was a lateral sidewall basilar artery aneurysm 2.5 cm in length with a wide 10-mm neck. Initially, the carotid-cerebral vascular system was infused with epoxy under fluoroscopic control. After recovering the brain and associated vessels during autopsy, the remaining cast of the arteries and aneurysm was used to create the vascular replicas by the lost wax technique. Details of this process have been described previously (11, 12). Again, four identical clear elastic silicone replicas were made from the original casting.

The experimental technique used for all models was as follows. The silicone replicas were placed in a circuit of pulsatile clear non-Newtonian fluid that mimics the rheologic properties of blood (13, 14). A blood pump (model 1421; Harvard

Apparatus Corp, S. Natick, MA) cycling at 1 pulse/s provided fluid flow. Flows were adjusted to replicate human physiologic flow profiles with a Square Wave Electromagnetic Flowmeter (Carolina Medical Electronics, Inc., King, NC), so that there was 40% forward flow during diastole as compared with flow during systole. Polyvinyl alcohol (PVA) particles were placed in the flowing fluid, and distance traveled (along the length of the vessel) over time was measured to calculate flow velocities. Fluid volume was measured in a graduated cylinder over time to determine flow volume. Before the experimental intravascular manipulations, we standardize the basilar artery flow volumes at 200 mL/min (0.003 L/s) and peak systolic velocities of 80 cm/s (0.8 m/s). These parameters were chosen to mimic those found in the normal human species. Specifically, for the flow velocity measurement, large (800–1000 μ) PVA particles were used; these could be visualized individually by digital video and by using digital video at 30 frames/s, to achieve a velocity of 80 cm/s, the particles travel 2.7 cm/frame.

Fluid slipstreams were opacified with dyes isobaric to the non-Newtonian fluid after insertion of 30-gauge needles through the vessel sidewall. Images were recorded on 35-mm film at shutter speeds up to 1/1000 of a second and on mini-DV digital video at shutter speeds up to 1/30 of a second. Images were obtained of the flow dynamics in the untreated vascular replica and after placement of a 4 \times 10-mm nondetachable balloon in the parent vessel at multiple locations surrounding the aneurysm neck, with varying degrees of inflation. Initially, the balloon was inflated to achieve 25% luminal diameter narrowing, followed by 50% and 75% luminal diameter narrowing, and finally complete vessel occlusion. Embolic occlusion was performed as determined by evaluation of the changes in the aneurysm flow dynamics with this initial placement of the nondetachable balloon. For liquid embolic deposition, a microcatheter was placed with the tip in the aneurysm sac, and the balloon was inflated to result in complete parent vessel occlusion. The liquid agent was then deposited very slowly into the aneurysm sac at a rate of 0.5 mL/min. Images were obtained while aneurysm embolization was performed of three models; first with the balloon proximal to the aneurysm neck, next across the aneurysm neck, and finally distal to the aneurysm neck. Images were also obtained in the other (fourth) identical model before treatment, after placement of a 4.5 \times 24-mm coronary stent (Magic Wallstent; Boston Scientific, Natick, MA) in the parent vessel across the aneurysm neck, and then after placement of a microcatheter through the stent mesh with the tip in the aneurysm to achieve liquid embolic occlusion of the aneurysm sac. Of note, this particular stent has a metallic surface area of 14%.

Results

In the untreated aneurysm replicas, undisturbed fluid slipstreams entered the distal portion of the aneurysm neck via a relatively small inflow zone, directed there by the junction of the aneurysm origin and parent vessel wall acting as a flow divider. The slipstreams impacted against the distal lateral aneurysm wall (also the point of aneurysm rupture in the cadaveric specimen). The slipstreams then swirled around the periphery of the aneurysm lumen, with a relatively slower velocity, in a reverse vortex pattern. Finally, the opacified slipstreams passed out the aneurysm neck, peripherally about the inflow zone (Fig 1A). Flow was similar during diastole, but less vigorous (9).

With the balloon partially inflated in the parent vessel, the slipstream velocity increased—a Bernoulli effect. This resulted in more rapid flow within the aneurysm sac, a less favorable condition for deposition of liquid embolic material (Fig 1B). The effect

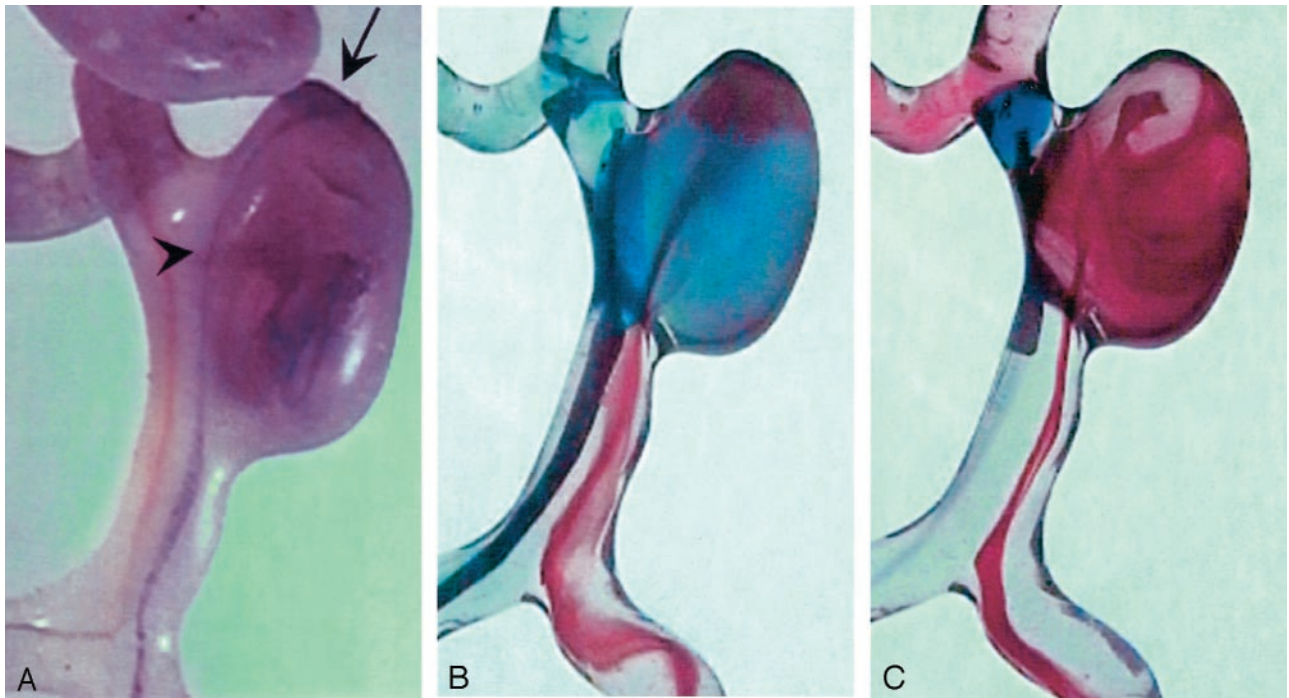


FIG 1. Cadaveric wide-necked basilar artery aneurysm replica of flow changes after parent vessel nondetachable balloon placement. A, In the unaltered replica, fluid slipstreams enter the aneurysm sac through the distal neck (arrowhead) and impact upon the distal lateral aneurysm wall (arrow), the site of aneurysm rupture in the cadaveric specimen. Flow swirls within the aneurysm sac and exits the aneurysm neck peripheral to the distal central incoming jet, usually at the proximal portion of the neck. B, Partial nondetachable balloon inflation, positioned in the parent vessel across the aneurysm neck, results in increased flow velocity of the intraaneurysmal fluid slipstreams, as well as greater impact against the aneurysm sidewall. C, Complete nondetachable balloon inflation results in stasis of the intraaneurysmal fluid slipstreams. Distal parent vessel balloon positioning shows intraaneurysmal slipstream opacification.

was more pronounced with greater degrees of balloon inflation (resulting in greater parent vessel narrowing) and when the balloon was proximal to the aneurysm neck compared with more distal parent vessel positioning. Whereas varying the needle position for isobaric dye injection opacified different flowing slipstreams, all the opacified slipstreams that entered the aneurysm sac demonstrated significant acceleration. Only with complete occlusion of the parent vessel lumen, either proximal to, across, or distal to the aneurysm sac, was there intraaneurysmal flow reduction (ie, stasis), a more favorable condition for liquid embolic material deposition (Fig 1C). Therefore, with parent vessel flow stasis, cyanoacrylate cement was then deposited and in all cases the polymer remained within the confines of the aneurysm sac. In addition, however, with the balloon positioned across the aneurysm neck, not only did the liquid agent remain in the aneurysm sac but due to the balloon protruding slightly (approximately 1–2 mm) into the aneurysm, a concave cement cast surface was molded which recreated a normal parent vessel lumen profile, resulting in the reestablishment of normal vascular flow patterns in the parent vessel (Fig 2).

After stent placement across the aneurysm neck, the intraaneurysmal flow changed significantly. Those slipstreams that did enter the aneurysm sac lost their coherence and, as they passed through the stent mesh, diffused generally into the center of the aneurysm. The previously noted rapid flow into the aneu-

rysm lumen appeared to decrease substantially, and the previously seen violent slipstreams impacting against the distal lateral aneurysm wall were no longer visualized (10, 15). None of the previously seen flow pattern remained (Fig 3A). During deposition of liquid embolic agent through the stent sidewall into the aneurysm sac, the stent mesh appeared to provide a barrier to passage of the embolic agent into the adjacent parent vessel, also a more favorable condition for liquid embolic material deposition (Fig 3B and C).

Discussion

In the last decade, there has been a greater appreciation of the necessity for understanding vascular flow dynamics, in particular of the intracranial arterial system, to further elucidate the pathophysiology of neurovascular disease processes (6–10, 15, 16). Generally, modeling of the cerebral vasculature or computer simulation has been performed for this purpose. However, laboratory-created models, while helpful, provide oversimplified versions of true human vascular physiologic properties. Likewise, computer simulation of three-dimensional fluid dynamics requires tremendous computer power, and usually assumptions must be introduced into the equations. Our approach has been to directly cast vessels from human cadaveric specimens, making anthropomorphic vascular replicas of high fidelity, and then plac-

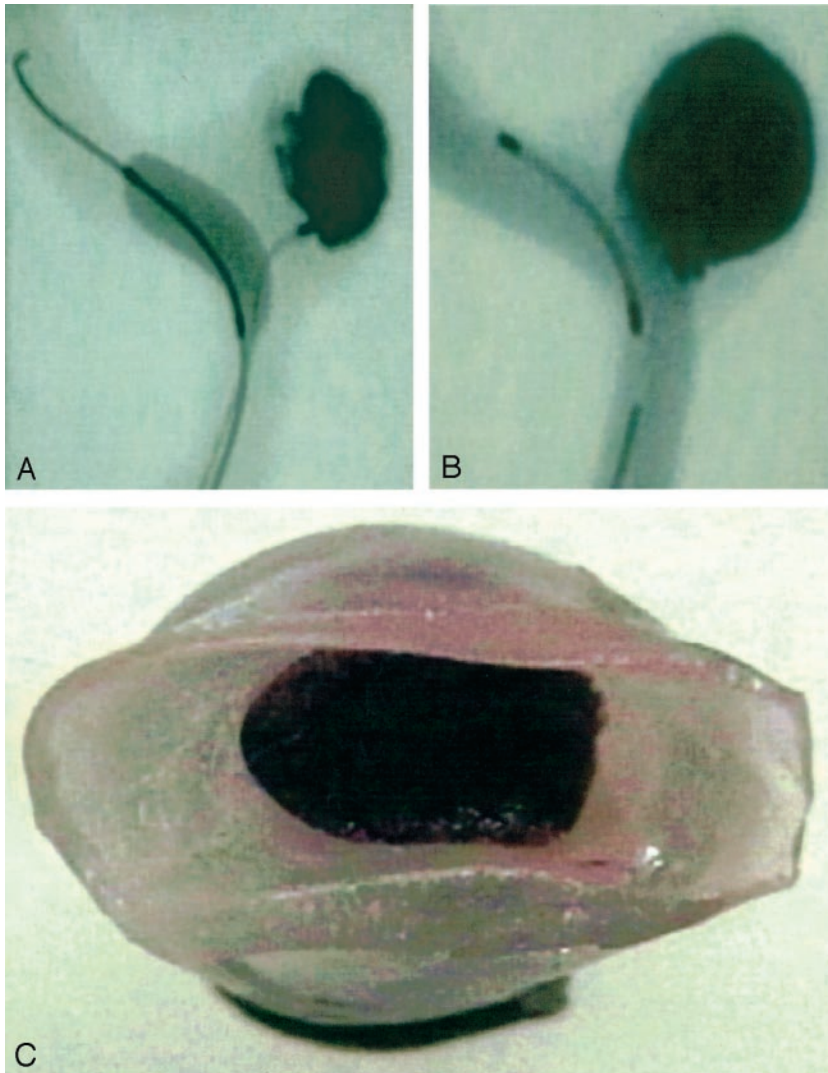


FIG 2. Laboratory-created wide-necked aneurysm model after treatment with parent vessel nondetachable balloon placement and cyanoacrylate deposition.

A, Fluoroscopic image of nondetachable balloon inflated within the parent vessel lumen across the aneurysm neck. Concomitant microcatheter tip placement within the aneurysm sac allows simultaneous cyanoacrylate deposition.

B, After completion of aneurysm occlusion, microwire withdrawal allows balloon deflation. The microcatheter has also been removed, and the parent vessel lumen is opacified with iodinated contrast material. This control angiogram shows no flow within the aneurysm.

C, Resected aneurysm model shows concave molding of the cement cast surface at the parent vessel-aneurysm interface, creating a cylindrical parent vessel surface profile.

ing those clear silicone elastic replicas in circuits of flowing fluid to directly observe the physiologic and pathophysiologic flow dynamics. Meticulous adjustment of the system is necessary to replicate the pulsatile flow found in human vessels, and our system corresponds to the flow velocity, volume, and profiles found at Doppler sonography (17). In addition, the value of the system was evident when with direct visualization the slipstreams were seen to impact upon the aneurysm's known cadaveric specimen rupture site, suggesting flow similar to that of the patient from which the replica was harvested.

It stands to reason that alteration of these pathologic slipstreams by means of endovascular devices, as well as (and possibly more importantly) the reestablishment of normal vascular flow patterns, should result in a more permanent treatment of the disease. Presently, the endovascular treatment of aneurysms is somewhat limited. The only device currently approved is the platinum detachable coil. Occasionally, incomplete occlusion or recanalization of the aneurysm is noted with this device usually in aneurysms with a wide neck or in those with large lumens (2, 3). Other embolization agents, such as cyanoacrylate ce-

ment, need to be developed that are noncompressible, more permanent devices which can also be used in conjunction with a parent vessel protection device to allow for the occlusion of these presently difficult to treat large and wide-necked aneurysms.

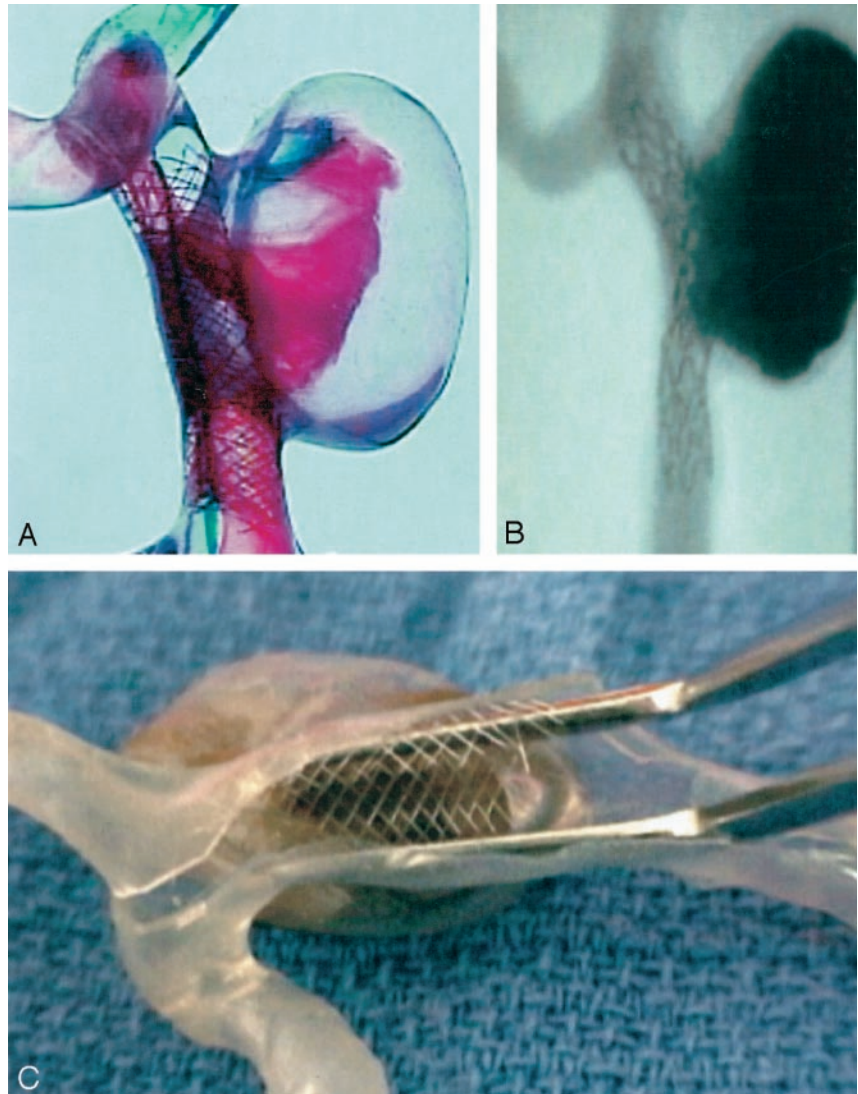
Use of the silicone nondetachable balloon for parent vessel protection is only feasible with complete vascular occlusion. This is due to the Bernoulli effect that is produced when the balloon is only partially occlusive. With partial balloon inflation, the flow velocity in the patent but narrowed remaining vascular lumen must increase to maintain a stable flow rate (ie, volume per unit time) (18, 19). Intraaneurysmal flow patterns became more disturbed with incremental increases in balloon inflation and subsequent increased vascular luminal narrowing. The effect was most pronounced when the balloon was placed across the aneurysm neck because of the direct effect of the parent vessel luminal narrowing on the adjacent aneurysm sac. With balloon placements proximal to the aneurysm neck, similar increased flow velocity and disturbed flow patterns are observed in the aneurysm sac since the vascular system is essentially a closed system and the effect is transmitted along the flowing

FIG 3. Wide-necked basilar artery aneurysm replica after treatment with parent vessel stent placement and subsequent cyanoacrylate occlusion.

A, Fluid slipstreams lose coherence as they pass through the stent mesh, with little, if any, impact against the aneurysm sidewall. The flowing slipstreams generally remain within the center of the aneurysm sac, and the intraaneurysmal reverse vortex flow pattern previously demonstrated has changed to a more disturbed flow profile.

B, Fluoroscopic image of completed cyanoacrylate occlusion of the aneurysm sac. Parent vessel lumen opacified with iodinated contrast material shows no flow within the aneurysm. (Note: this particular image shown for descriptive purposes was taken from a different experimental embolization with use of an AVE stent.)

C, Resected aneurysm replica shows no evidence of cement penetration through the stent mesh.



fluid cylinder. Interestingly, the effect is also noted with balloon placements distal to the aneurysm neck, although less pronounced degrees of increased disturbed flow are seen. Therefore, complete parent vessel occlusion is required to prevent development of this increased flow velocity and these disturbed flow patterns that are detrimental for safe liquid embolic deposition. However, even with vessel occlusion and complete vascular stasis, liquid embolic material could potentially still enter the parent vessel with the proximal or distal aneurysm neck balloon positioning. Maximal safety is thus achieved with the balloon placed completely across the aneurysm neck and inflated to the point of luminal occlusion. With this configuration and a microcatheter tip simultaneously positioned in the aneurysm sac, liquid embolic agent can then be safely deployed.

An additional benefit of this approach is that the inflated balloon across the aneurysm neck mimics the shape of the original parent vessel lumen and will shape the intraaneurysmal cement cast with a concave border at the aneurysm sac–parent vessel interface. This result is much more easily achieved with a highly

malleable agent such as cyanoacrylate cement compared with platinum detachable coils. This important secondary effect results in reestablishment of normal parent vessel flow dynamics and may aid in reducing the chance of aneurysm reformation since many investigators now assume initial aneurysm formation may be based on de novo abnormal parent vessel flow patterns (20–24).

This technique, however, has two potential problems. Since the aneurysm sac becomes a “closed compartment” with complete parent vessel occlusion across the aneurysm neck, intraaneurysmal pressure may increase during liquid deposition, possibly leading to aneurysm rupture. Experimentation is currently being performed to measure this pressure change and the extent of aneurysm sac exclusion with balloon inflation, in particular with the use of low-compliance silicone balloons. Although one may wish to prevent this situation by using partial balloon inflation, as described, the partial balloon inflation technique leads to increased intraaneurysmal flow and a greater chance of untoward parent vessel cement extravasation during intraaneurysmal cyanoacrylate deposition. Like-

wise, whereas proximal or distal balloon positioning can induce vascular stasis with complete balloon inflation, cement may still potentially extravasate from the aneurysm sac without complete coverage across the aneurysm neck. Although this extravasation was not noted in our limited number of embolizations, this method could result in unnecessary patient risk.

The other issue with the prescribed technique is that the balloon is in direct contact with the cyanoacrylate and may become affixed to the cement as it polymerizes. Silicone, however, should not adhere to the cyanoacrylate polymer, and this has been our experience in the laboratory, although theoretically, this could also be a concern with in vivo use.

A second potential technique is to cross the aneurysm neck with a stent. Stent placement is presently limited by the difficulty in traversing the bends in the carotid and vertebral arteries, as well as those in the proximal intradural vessels, but already, clinical success has been achieved (25–27). Our finding of placing a mesh stent across the aneurysm neck, which dramatically decreases the velocity of the slipstreams flowing into the aneurysm sac, also results in a satisfactory condition for the safe deposition of a liquid embolic agent. It was relatively straightforward to insert a microcatheter through the stent mesh and into the aneurysm lumen for the subsequent delivery of the cyanoacrylate. During deposition, the cement remained within the aneurysm sac owing to the stent mesh acting as a barrier preventing passage of the cement into the adjacent parent vessel even though the stent has a porous structure. In addition, the intrinsic cylindrical stent configuration also re-creates a normal parent vessel lumen and reestablishes a normal parent vessel flow profile. Finally, unlike the nondetachable balloon technique, given the porous structure of the stent and the permanent deployment of the device, the previously described potential complications such as intraaneurysmal pressure changes or stent-cement adherence are no longer of concern.

In all, the creation of replicas of human vascular abnormalities, particularly aneurysms, is a tedious and technically difficult challenge, but allows a more complete and deeper understanding of the initial pathologic vascular flow dynamics and the subsequent design of better treatment paradigms for this often lethal disease.

Conclusion

From this laboratory experimentation, the knowledge gained of aneurysm flow dynamics and changes incurred after endovascular parent vessel flow alteration provides a basis for the future feasibility of aneurysm obliteration by using a liquid embolic agent with a neurointerventional technique.

References

1. Eskridge JM, Song JK. Endovascular embolization of 150 basilar tip aneurysms with Guglielmi detachable coils: results of the Food and Drug Administration multicenter clinical trial. *J Neurosurg* 1998;89:81–86
2. Guglielmi G, Vinuela F, Duckwiler G, et al. Endovascular treatment of posterior circulation aneurysms by electrothrombosis using electrically detachable coils. *J Neurosurg* 1992;77:515–524
3. Vinuela F, Duckwiler G, Mawad M. Guglielmi detachable coil embolization of acute intracranial aneurysm: perioperative anatomical and clinical outcome in 403 patients. *J Neurosurg* 1997;86:475–482
4. Sluzewski M, Menovski T, van Rooij WJ, Wijnalda D. Coiling of very large or giant cerebral aneurysms: long-term clinical and serial angiographic results. *AJNR Am J Neuroradiol* 2003;24:257–262
5. Fournier D, TerBrugge KG, Willinski R, et al. Endovascular treatment of intracerebral arteriovenous malformations: experience in 49 cases. *J Neurosurg* 1991;75:228–233
6. Brothers MF, Kaufmann JCE, Fox AJ, Deveikis JP. N-butyl-2-cyanoacrylate: substitute for IBCA in interventional neuroradiology—histopathologic and polymerization time studies. *AJNR Am J Neuroradiol* 1989;10:777–786
7. Chong BW, Kerber CW, Buxton RB, et al. Blood flow dynamics in the vertebrobasilar system. *AJNR Am J Neuroradiol* 1994;15:733–745
8. Liou TM, Chang WC, Liao CC. Experimental study of steady and pulsatile flows in cerebral aneurysm model of various sizes at branching site. *J Biomech Eng* 1997;119:325–332
9. Imbesi SG, Kerber CW, Knox K. Analysis of slipstream flow in two ruptured intracranial cerebral aneurysms. *AJNR Am J Neuroradiol* 1999;20:1703–1705
10. Imbesi SG, Kerber CW. Analysis of slipstream flow in a wide-necked basilar artery aneurysm: evaluation of potential treatment regimens. *AJNR Am J Neuroradiol* 2001;22:721–724
11. Kerber CW, Heilman CB, Zanetti PH. Transparent elastic arterial models, I: a brief technical note. *Biorheology* 1989;26:1041–1049
12. Liepsch D, Zimmer R. A method for the preparation of true-to-scale inflexible and natural elastic human arteries. *Biomed Tech* 1978;23:227–230
13. Mann DE, Tarbell JM. Flow of non-Newtonian blood analog fluids in rigid curved and straight artery models. *Biorheology* 1990;27:711–733
14. Liepsch D, Morabec ST. Pulsatile flow of non-Newtonian fluid in distensible models of human arteries. *Biorheology* 1984;21:571–586
15. Aenis M, Stancampiano AP, Wakhloo AK, Lieber BB. Modeling of flow in a straight stented and non-stented side wall aneurysm model. *J Biomech Eng* 1997;119:206–212
16. Burleson AC, Strother CM, Turitto VT. Computer modeling of intracranial saccular and lateral aneurysms for the study of their hemodynamics. *Neurosurgery* 1995;37:774–782
17. Keller HM, Merer WE, Anliker M, et al. Non-invasive measurement of velocity profiles and blood flow in the common carotid artery by pulsed Doppler ultrasound. *Stroke* 1976;7:370–377
18. Berne RM, Levy MN. Hemodynamics. In: *Physiology*. St. Louis: Mosby, 1983:473–484
19. Serway RA. *Physics for Scientists & Engineers*, 4th ed. Philadelphia: W. B. Saunders, 1996:433–435
20. Hashimoto N, Handa H, Hazama F. Experimentally induced cerebral aneurysms in rats. *Surg Neurol* 1983;19:107–111
21. Kim C, Kikuchi H, Hashimoto N, Hazama F. Histopathological study of induced cerebral aneurysms in primates. *Surg Neurol* 1989;32:45–50
22. Crompton MR. Mechanisms of growth and rupture in cerebral berry aneurysms. *BMJ* 1966;1:1138–1142
23. Kim C, Cervos-Navarro J, Patzold C, Tokuriki Y, Takebe Y, Hori K. In vivo study of flow pattern at human carotid artery bifurcation with regard to aneurysm development. *Acta Neurochir* 1992;115:112–117
24. Greenhill NS, Stehbins WE. Scanning electron-microscopic study of experimentally induced intimal tears in rabbit arteries. *Atherosclerosis* 1983;49:119–126
25. Wilms G, van Calenbergh F, Stockx L, Demaerel P, van Loon J, Goffin J. Endovascular treatment of a ruptured paraclinoid aneurysm of the carotid siphon achieved using endovascular stent and endosaccular coil placement. *AJNR Am J Neuroradiol* 2000;21:753–756
26. Sekhon LHS, Morgan MK, Sorby W, Grinnell V. Combined endovascular stent implantation and endosaccular coil placement for the treatment of a wide-necked vertebral artery aneurysm: technical case report. *Neurosurgery* 1998;43:385–388
27. Lanzino G, Wakhloo AK, Fessler RD, Hartney ML, Guterman LR, Hopkins LN. Efficacy and current limitations of intravascular stents for intracranial internal carotid, vertebral, and basilar artery aneurysms. *J Neurosurg* 1999;91:539–547